Modelling breakage and reagglomeration during fine dry grinding in ball milling devices

S. Fadda, A. Cincotti, G. Cao

Dipartimento di Ingegneria Chimica e Materiali, Università degli Studi di Cagliari, Piazza d'Armi, 09123 Cagliari, Italy

Modelling of grinding of fine powders in ball milling devices is addressed. The model quantitatively describes breakage and agglomeration phenomena by considering two populations, i.e. primary particles and porous aggregates. The population balance approach takes into account breakage and aggregation kernels which are considered functions of the size of the two populations. The proposed model is able to properly simulate the inversion from the breakage to the agglomerative regime typical of fragile material powder system undergoing ball milling. A suitable fitting procedure is performed for separately determining the adjustable parameters of the model. Model reliability is tested against experimental data, while the proposed breakage/agglomeration kernels are related to the quantitative description of ball milling apparatus dynamics.

1. Introduction

Several areas of chemical and pharmaceutical industries as well as of the ceramic and microelectronic ones make use of sub-micron particles. It is well known that the manufacturing of fine particles may be effectively achieved by means of grinding processes such as ball milling (BM). However, when particle sizes are reduced to values smaller than 1 μm, aggregation may take place, thus contrasting breakage phenomena. Particle size increasing during fine grinding of silicates has been experimentally recognized by Opoczky in 1977, who stated that aggregation represents a phenomenon characterized by the weak, reversible adhesion of particles due to Van der Waals forces. It is worth noting that, aggregation phenomenon is usually considered non-productive and grinding aids are adopted to avoid its occurrence. However, Ho and Hersey in 1979 proposed to exploit the agglomerative phase to produce pharmaceutical granules in rotating or oscillating ball mills. More recently, Le Bolay investigated the possibility of obtaining an homogeneous aggregative dispersion of grinded particles into a matrix, thus synthesizing composite materials via BM (Le Bolay, 2003). In all these papers, the temporal transition from a regime dominated by breakage to that one dominated by agglomerative (aggregative) phenomena is experimentally evidenced by cumulative distribution curves which move back and forth (inversion), and/or by an average diameter which shows a minimum as time proceeds. Control and scaling-up procedures of this particular behaviour of grinding processes may be supported by the development of reliable mathematical models based on first principles of conservation. The aim of
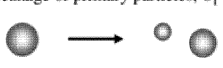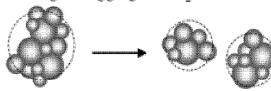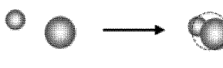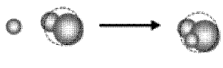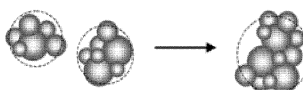
such approach is to minimise the economic effort related to experimental campaigns driven by a trial & error procedure. It is worth noting that attempts towards quantitative analysis and modelling, based on the population balance approach, of simultaneous breakage and reagglomeration phenomena in milling processes, have been relatively rare. In this work, on the basis of the two populations approach adopted by Kaya et al. (1997), a mathematical model able to describe the inversion from breakage to agglomerative regime taking place in BM devices is developed. In particular, breakage and aggregation kernels which depend on the size of the two particle populations are proposed. A proper fitting procedure is performed in order to independently determine the adjustable parameters of such kernels. While testing model reliability against suitable experimental data, the proposed breakage/agglomerative kernels are also related to the quantitative description of BM apparatus dynamics recently presented in the literature (Concas et al., 2006).

2. Model equations

In this work, a 1-D PBE formulation is adopted for two distinct particle populations, i.e. primary particles (n_1) and aggregates of primary particles (n_2). Particle volume is chosen as internal coordinate while the proposed model is formulated on the basis of constant density powders. Thus, volume conservation is guaranteed. Breakage and aggregation phenomena taken into account are depicted in Table 1. As it can be seen, breakage and aggregation phenomena are interpreted as first or second order reactions. By assuming that spherical shaped particles are uniformly distributed along the miller volume, the PBEs considered for each particle populations are reported in Table 1 (cf. eqs. (1) and (2)) along with the mathematical expressions for birth and death terms appearing therein. Specifically, $\alpha_{i,j}$, β_i and β_i' (with $i = 1,2$ and $j = 1,2$) represent aggregation and breakage kernels. Analogously to chemical reaction kinetics, in the breakage kernel the *selection function*, $K_{b_i}(\varepsilon)$, represents the reaction constant, while the *transfer function*, $b(v,\varepsilon)$, corresponds to the stoichiometric coefficient, i.e. the number of daughter particles of volume v produced by breakage of one single mother particle of volume ε. As for any chemical reaction constant, the selection function (representing the breakage probability, per unit time, for one mother particle to impact with the milling bodies) can be expressed as the product of two probabilities (cf. Eq. 10), namely $K_{b_i}^0$ (i.e. the frequency of impacts, which depends on the dynamics of the process), and $E_{b_i}(\varepsilon)$ (i.e. the probability that one impact is efficient). h_{b_i}, the adjustable parameter characteristic of the specific material at hand, identifies a lower limit for particles reduction by comminution. Below a certain volumic size, breakage phenomena do not take place since impact efficiency is too low. Analogously to the breakage kernel formulation (cf. eqs. (8)-(12)), the aggregation kernel is expressed as the product between two terms representing frequency and efficiency of aggregation impact, as stated in eq. (13). However, the impact frequency of the aggregation kernel depends not only on dynamics, but also on the size of the two aggregating particles (v and ε), by means of the factor $a(v,\varepsilon)$ (cf. eq. 15). Here, the *cross-sectional area* (CSA) kernel is

assumed so that impact frequency for aggregation increases as the sizes of the aggregating particles increase. Regarding the aggregation efficiency, $E_{a_{i,j}}(v+\varepsilon)$, expressed by eq. (16), introduces the adjustable parameter $h_{a_{i,j}}$ which depends on the specific material.

Table 1 Model equations.

Population Balance Equations		
$\dfrac{\partial n_1(v,t)}{\partial t}=B_{b_1}-D_{b_1}-D_{a_{11}}-D_{a_{12}}$	$@\ t=0\quad n_1(v)=n_1^0(v)$	(1)
$\dfrac{\partial n_2(v,t)}{\partial t}=B_{b_2}-D_{b_2}+B_{a_{11}}+B_{a_{12}}-D_{a_{12}}+B_{a_{22}}-D_{a_{22}}$	$@\ t=0\quad n_2(v)=0$	(2)

Birth and Death terms of breakage and aggregation phenomena		
$B_{b_1}=\displaystyle\int_v^\infty \beta_1(v,\varepsilon)\cdot n_1(\varepsilon,t)\cdot d\varepsilon$ (3a) $D_{b_1}=\beta_1'(v)\cdot n_1(v,t)$ (3b)	Breakage of primary particles, b_1 $n_1(v)\to n_1(v-\varepsilon)+n_1(\varepsilon)$	
$B_{b_2}=\displaystyle\int_v^\infty \beta_2(v,\varepsilon)\cdot n_2(\varepsilon,t)\cdot d\varepsilon$ (4a) $D_{b_2}=\beta_2'(v)\cdot n_2(v,t)$ (4b)	Breakage of aggregates, b_2 $n_2(v)\to n_2(v-\varepsilon)+n_2(\varepsilon)$	
$B_{a_{11}}=\dfrac{1}{2}\cdot\displaystyle\int_0^v \alpha_{11}(v-\varepsilon,\varepsilon)\cdot n_1(v-\varepsilon,t)\cdot n_1(\varepsilon,t)\cdot d\varepsilon$ (5a) $D_{a_{11}}=n_1(v,t)\cdot\displaystyle\int_0^\infty \alpha_{11}(v,\varepsilon)\cdot n_1(\varepsilon,t)\cdot d\varepsilon$ (5b)	Aggregation between primary particles, a_{11} $n_1(v-\varepsilon)+n_1(\varepsilon)\to n_2(v)$	
$B_{a_{12}}=\displaystyle\int_0^v \alpha_{12}(v-\varepsilon,\varepsilon)\cdot n_1(v-\varepsilon,t)\cdot n_2(\varepsilon,t)\cdot d\varepsilon$ (6a) $D_{a_{12}}=n_1(v,t)\cdot\displaystyle\int_0^\infty \alpha_{12}(v,\varepsilon)\cdot n_2(\varepsilon,t)\cdot d\varepsilon$ (6b) $D_{a_{12}}=n_2(v,t)\cdot\displaystyle\int_0^\infty \alpha_{12}(v,\varepsilon)\cdot n_1(\varepsilon,t)\cdot d\varepsilon$ (6c)	Aggregation between primary particles and aggregates, a_{12} $n_1(v-\varepsilon)+n_2(\varepsilon)\to n_2(v)$	
$B_{a_{22}}=\dfrac{1}{2}\cdot\displaystyle\int_0^v \alpha_{22}(v-\varepsilon,\varepsilon)\cdot n_2(v-\varepsilon,t)\cdot n_2(\varepsilon,t)\cdot d\varepsilon$ (7a) $D_{a_{22}}=n_2(v,t)\cdot\displaystyle\int_0^\infty \alpha_{22}(v,\varepsilon)\cdot n_2(\varepsilon,t)\cdot d\varepsilon$ (7b)	Aggregation between aggregates, a_{22} $n_2(v-\varepsilon)+n_2(\varepsilon)\to n_2(v)$	

Breakage kernel	Aggregation kernel
$\beta_i(v,\varepsilon)=b(v,\varepsilon)\cdot K_{b_i}(\varepsilon)\qquad i=1,2$ (8) $\beta_i'(v)=K_{b_i}(v)\qquad i=1,2$ (9) $K_{b_i}(\varepsilon)=K_{b_i}^0\cdot E_{b_i}(\varepsilon)\qquad i=1,2$ (10) $E_{b_i}(\varepsilon)=\left[1-\exp\!\left(-\dfrac{\varepsilon}{h_{b_i}}\right)\right]\qquad i=1,2$ (11) $b(v,\varepsilon)=\dfrac{2}{\varepsilon}$ (12)	$\alpha_{i,j}(v,\varepsilon)=K_{a_{i,j}}^0(v,\varepsilon)\cdot E_{a_{i,j}}(v+\varepsilon)\qquad i,j=1,2$ (13) $K_{a_{i,j}}^0(v,\varepsilon)=k_{a_{i,j}}^0\cdot a(v,\varepsilon)\qquad i,j=1,2$ (14) $a(v,\varepsilon)=\left(v^{1/3}+\varepsilon^{1/3}\right)^2$ (15) $E_{a_{i,j}}(v+\varepsilon)=\exp\!\left(-\dfrac{(v+\varepsilon)}{h_{a_{i,j}}}\right)\qquad i,j=1,2$ (16)

Basically, eq. (16) identifies an upper limit to the size of the aggregate with volume $(v+\varepsilon)$, above which impact efficiency drops down to zero, thus preventing the aggregation phenomena to occur. On the contrary, the maximum efficiency is obtained

when smaller particles collide. The model consisting of the system of integro-differential eqs. (1)-(16), takes into account five different phenomena (two types of breakage and three types of agglomeration, respectively), each of them introducing two adjustable parameters (one impact frequency and one efficiency volume). This model is numerically solved by means of PARSIVAL (Cit GmbH, Germania), a commercial software based on finite elements (h-p Galerkin), which automatically adapts the temporal and size internal coordinate grids in response to the stiffness of the problem and the requested accuracy of its solution.

3. Results and discussion

In Figures 1a-1b the experimental evidence of the inversion occurring during the BM of a sandy soil powder is reported. Briefly, 4 g of sandy soil (i.e. silica 78 w% and bentonite 22 w%) are treated in the $65\ cm^3$ grinding chamber of the Spex Mixer/Mill mod. 8000. This apparatus is operated at 1425 rpm, with only one milling ball corresponding to a charge ratio equal to 2 . More details on the experimental set-up and the powder system preparation are reported in the literature (Concas et al., 2006; Concas et al., 2007; Fadda et al., 2009). Specifically, in Figure 1a the temporal transition from the breakage to the agglomeration phase in terms of mass percentage cumulative distribution curves M (at different BM times), experimentally measured by means of a CILAS 1180 laser granulometer, may be clearly seen. On the basis of these curves, the corresponding temporal profile of the volumic mean diameter (D_{4_3}) is calculated and reported in Figure 1b. As can be seen, an agglomerative phase becomes dominating after about 0.5÷1 h of comminution which initially produces a reduction on particles' size. From these experimental results, it may be reasonably assumed that two populations of particles are generally present inside the milling device. Specifically, only primary particles n_1 are initially present, as considered by the developed model (i.e. initial conditions of eqs. (1) and (2). Weak aggregates n_2 are formed only after an initial breakage of primary particles, presumably by the action of Van der Waals forces. On the basis of these considerations, a reliable independent determination of the ten unknown parameters has been performed by interpreting experimental data at increasing BM times through a progressively more complex version of the model reported in Table 1. Details on the parameter estimation procedure specifically adopted are given elsewhere (Fadda et al., 2009). The values of the ten unknown parameters obtained following this procedure are reported in Table 2, while the comparison between experimental data and model results is given in Figures 2b-c in terms of the mass percentage density distribution curves m. The adopted regression procedure consists of numerical minimization along adjustable model parameters of a cost function made by summing up the quadratic errors between the experimental and calculated values of m. In Figures 2b-c, the corresponding model predictions in terms of mass percentage cumulative distribution curves M are also reported. As it can be seen matching is good. Model reliability is further tested in Figure 2d where model predictions of the two curves are compared with the corresponding experimental data after 3 h of BM processing.

It is worth noting that, the fitted value for $K_{b_1}^0$ reported in Table 2 fairly agrees with that one (i.e. 2.04) obtainable by applying the *method of initial rates* to the larger particles of n_1 population, as proposed by Micco et al. (2000). In addition, by means of the model for simulating the 3-D dynamics of the milling bodies recently proposed by Concas *et al.* (2006), a value of 2.574 h^{-1} for $K_{b_1}^0$ may be successfully predicted. Same considerations hold for $K_{b_2}^0$.
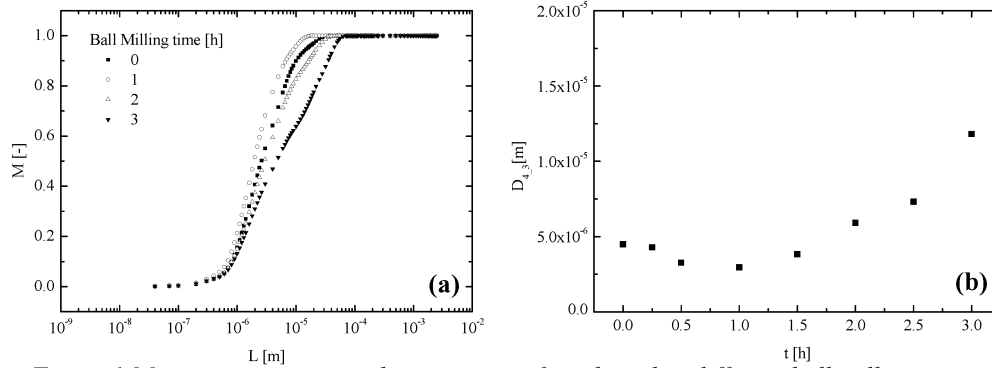

Figure 1 Mass percentage cumulative curves of sandy soil at different ball milling times (a) and volumic mean diameter of sandy soil as a function of ball milling time (b).

Table 2 Model parameters.

Parameter	Value	Dimension	Parameter	Value	Dimension
$K_{b_1}^0$	2.638	h^{-1}	h_{b_1}	$1.141 \cdot 10^{-21}$	m^3
$K_{b_2}^0$	2.524	h^{-1}	h_{b_2}	$3.620 \cdot 10^{-22}$	m^3
$k_{a_{11}}^0$	$2.155 \cdot 10^{-6}$	m h^{-1}	$h_{a_{11}}$	$3.342 \cdot 10^{-21}$	m^3
$k_{a_{12}}^0$	$2.514 \cdot 10^{-3}$	m h^{-1}	$h_{a_{12}}$	$2.508 \cdot 10^{-19}$	m^3
$k_{a_{22}}^0$	$2.471 \cdot 10^{-3}$	m h^{-1}	$h_{a_{22}}$	10^{-10}	m^3

This result confirms once again the reliability of the proposed model as well as the adopted fitting procedure. Since the parameters h_{b_i} ($i = 1,2$) are material-dependent, their values cannot be estimated a priori. Nevertheless, it is worth noting that, the value of h_{b_1} results from the fitting procedure lower than that of h_{b_2} (cf. Table 2). This seems a reasonable result since, according to eq. (11), it means that primary particles n_1 are harder to break than agglomerates n_2. On the other hand, it is not possible to relate the impact frequencies for agglomeration phenomena (i.e. the constants $k_{a_{11}}^0$, $k_{a_{12}}^0$, and $k_{a_{22}}^0$) to the dynamics of the milling device. Presumably, this is due to the fact that the actual agglomerative impact event is not binary as assumed by the model (cf. Table 1). Regarding to the volumic upper limit of agglomeration efficiencies ($h_{a_{11}}$ and $h_{a_{12}}$), the fitted values of these material-dependent parameters are relatively low, i.e. corresponding to a linear dimension of 10^{-7} and 4x10^{-7} m, respectively. Therefore,

considering the initial mass percentage density distribution curve reported in Figure 2a, it is apparent that a relatively fine powder needs to be reached by breakage before agglomeration may effectively take place. This is a crucial aspect of the proposed model for the mathematical description of the transition from breakage to agglomeration regime. An higher value is obtained, instead, for the material-dependent parameter $h_{a_{22}}$, so that the efficiency factor in eq. (16) may be actually neglected for the case of aggregation a_{22}.
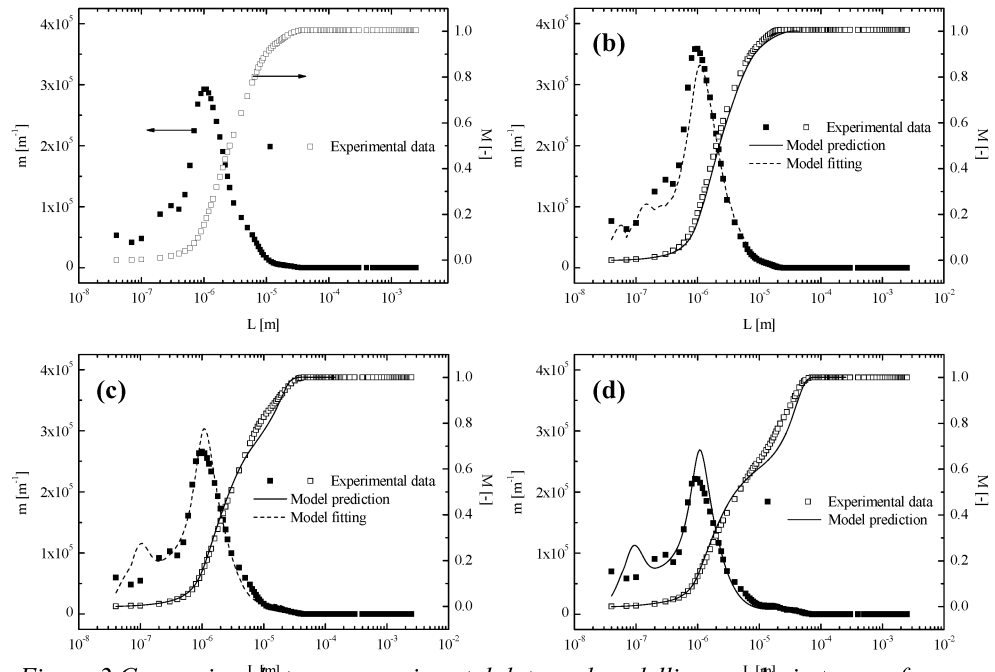

Figure 2 Comparison between experimental data and modelling results in terms of mass percentage cumulative and density distribution curves at different ball milling time: 0 (a), 30 min (b), 2 h (c), 3 h (d).

References

Concas, A., N., Lai, M., Pisu, G., Cao, 2006. Modelling of comminution process in Spex Mixer/Mill. *Chemical Engineering Science*. 61, 3746-3760.

Concas A., Montinaro S., Pisu M., Cao G., 2007. Mechanochemical remediation of heavy metals contaminated soils: modelling and experiments. *Chemical Engineering Science*. 62, 5186-5192.

Fadda S., A., Cincotti, G., Cao, 2009. Modelling breakage and reagglomeration during fine dry grinding in Spex Mixer/Mill, *Powder Technology*, submitted for publication.

Ho, T., J.A., Hersey, 1979. Granulation using the agglomerative phase of comminution. *Powder Technology*. 23, 191-195.

Kaya, E., H., Cho, R., Hogg, 1997. Reagglomeration in fine dry grinding of coal. *Mineral and Metallurgical Processing*. 37-42.

Le Bolay, N., 2003. On agglomeration phenomena in ball mills: application to the synthesis of composite materials. *Powder Technology*. 52, 450-455.

Micco, G., P.A., Netti, L., Nicolais, A., Collina, G., Astarita, 2000. A novel approach for grinding operation scale-up. *Chemical Engineering Science*. 55, 1347-1356.

Opoczky, L., 1977. Fine grinding and agglomeration of silicates. *Powder Technology*. 17, 1-7.